Ionospheric and Plasmaspheric Contribution to the Total Electron Content Inferred from Ground Data and Radio-Occultation-Derived Electron Density

G. González-Casado, J. M. Juan, J. Sanz, A. Rovira-García,
Research Group of Astronomy and Geomatics, Technical University of Catalonia (gAGE/UPC), Spain

and A. Aragon-Angel
European Commission Joint Research Center (JRC), Italy

BIOGRAPHIES

Dr. G. González-Casado is senior researcher at gAGE/UPC. His current research interests are: analysis and modeling of the ionosphere and plasmasphere based on GNSS observations and data from radio occultations; high accuracy GNSS Navigation; and satellite-based and ground-based Augmentation Systems.

Dr. J.M. Juan Zornoza is senior researcher at gAGE/UPC. His current research interests are in the area of GNSS data processing Algorithms for High Accuracy GNSS Navigation and GNSS ionospheric sounding, as well as Augmentation Systems (SBAS and GBAS).

Dr. J. Sanz Subirana is senior researcher at gAGE/UPC. His current research interests are in the area of GNSS data processing algorithms, GNSS ionospheric sounding, augmentation systems (SBAS and GBAS), and High Accuracy GNSS Navigation.

A. Rovira-García is currently pursuing a PhD in the Aerospace Science and Technology Doctoral Program of UPC. In January 2012 he was granted a PhD. co-sponsorization fellowship together with the industrial partner FUGRO by the European Space Agency. Since then his research is focused in enhanced algorithms related with the real-time Fast-PPP technique.

Dr. A. Aragon-Angel is a scientific/technical officer at the Joint Research Center (JRC) of the European Commission (EC), Italy. Her working topics range from ionospheric radio occultation to precise positioning and navigation within the area of GNSS data processing.

ABSTRACT

The performance of a new method allowing the determination of the separate contributions from the ionosphere and the plasmasphere to ground measurements of the vertical total electron content (VTEC) is demonstrated. After introducing and testing the proposed method, a preliminary global-scale analysis of the ionosphere-plasmasphere system during a period of low solar activity is presented. The results show some regular features in the seasonal, geomagnetic latitude and local time variations of the fractional ionospheric electron content. These features are modeled by means of a simple fitting function allowing also the characterization of the fractional plasmaspheric contribution to the VTEC.

INTRODUCTION

Usually, for Global Navigation Satellite System (GNSS) applications, the ionosphere is modeled as a single layer located at a fixed altitude representative of that region [1]. However, this approach disregards the contribution from the plasmasphere (a region extending toward heights of several thousands of kilometers) to slant total electron content measurements. Previous studies have shown that this contribution is not negligible, especially during the night [2]. Hence, the characterization of the ionosphere-plasmasphere electron content is of great importance to achieve a precise modeling of the GNSS signal delays. Taking advantage of the nearly world-wide coverage of both radio occultations from the COSMIC/FORMOSAT-3 (CF3) constellation and the global ionospheric maps (GIMs) [3] from the International GNNS Service (IGS), this study presents a methodology that self-consistently combines all these available data to achieve a reliable determination of the electron contents in the ionospheric and plasmaspheric regions separately.

Measurements from GNSS receivers on board CF3 satellites during radio occultation (RO) of global positioning system (GPS) satellites can be used to derive altitude-dependent electron density profiles at least up to the typical altitude of the CF3 satellites (750-800 km). Since the profiles sample most of the F-region under normal conditions, one can estimate the vertical electron

content contributed by the ionosphere by direct integration of the profile over the range of altitudes covered by the RO measurements. However, the altitude of the CF3 satellites does not represent, in general, the true upper limit of the ionosphere. The particular altitude marking the transition from the ionosphere to the plasmasphere, usually called the upper transition height (UTH), depends on the different physical conditions affecting the ionosphere-plasmasphere system at different periods of the day, seasons of the year, geographic locations and solar and geomagnetic activity.

Therefore, instead of using the satellite altitude to separate the ionospheric and plasmaspheric electron contents, the simplified topside ionosphere plus protonosphere (STIP) model [4] is used to describe the RO-retrieved electron density profile in the altitude range from a few tens of kilometers above the F2-peak to nearly the CF3 satellite altitude, typically corresponding to the topside ionosphere region. The model assumes that the electron content in this range of altitudes can be represented by the sum of two terms accounting for the density of the two major constituent ions of the region, O^+ and H^+. Using this model, the electron content contributed by the ionosphere above the CF3 satellite altitude can be accounted for and, moreover, the interplay between the ionosphere and plasmasphere under different physical conditions is reproduced in a more realistic way.

This model-fitting strategy is applied to the electron density profiles retrieved from ROs by means of an improved Abel transform (IAT) methodology [5] that takes into account the horizontal gradients in the electron density by using externally provided VTEC values. Contrary to the most conventional approach (known as classical Abel transform inversion), which assumes local spherical symmetry, the IAT method achieves more precise results when compared with ionosonde measurements [6].

In this study, after firstly describing the particular data sample that will be analyzed, the details of the methodology to separate the VTEC into the ionospheric and plasmaspheric contributions are introduced. Then, the performance of the method is demonstrated by reproducing previously observed properties of the ionosphere and the plasmasphere during the period of time covered by the analysis. In particular, it is shown that the method can be used to analyze general trends characterizing the ionosphere-plasmasphere interplay. In the last two sections, the results are discussed and the conclusions and some future applications are presented.

RADIO-OCCULTATION OBSERVATIONS

The CF3 constellation consists of six low Earth orbit (LEO) satellites that measure GPS signals during ROs. For the present study, the observations considered were taken during two years belonging to the last solar minimum period, 2007 and 2009. Typically one day per week was selected during 2007 and one day per month during 2009. In the two years the selected days were evenly spaced. Since the orbits of the CF3 satellites change slowly from day to day, this procedure avoids the accumulation of redundant data while providing reasonably dense coverage of all geographic locations around the globe. In this way, a nearly worldwide analysis of the ionospheric and plasmaspheric electron contents can be performed, which allows testing the results of the methodology proposed in this study.

RO observations that did not sampled altitudes from 200 to 700 km were discarded from the data set. More than 70,000 ROs were finally selected after processing raw data from the COSMIC Data Analysis and Archive Center (CDAAC). The two years covered by the data sample were part of a particularly long and deep solar minimum, lasting over 4 years (from 2007 to 2010). Specifically, during 2007, the 10.7 cm solar flux index, F10.7, was always smaller than 95 solar flux units (sfu), and it only reached values over 80 sfu less than 20% of the time. The solar activity during 2009 was even lower since it was the year of minimum activity during the last solar cycle period. Additionally, periods of strong geomagnetic activity were very scarce, values of the magnetic activity index, K_p, greater than 4 rarely occurred during the days included in our sample, and the duration of such events was short.

Finally, in order to include the effects of horizontal gradients in the electron density profile retrievals from ROs, VTEC values for the time intervals corresponding to RO measurements were collected from the GIMs provided by IGS [3] and subsequently interpolated to the different geographical locations covered by each RO in the sample.

METHOD

Electron density profile

The IAT [5] has been used to retrieve electron density profiles from our data sample of RO measurements. The IAT method is an inversion method targeted to the determination of a shape function, $F(h)$, depending only on the altitude h and characterizing the height variation of the electron density, N_e, which according to the separability hypothesis used by the IAT, can be expressed as the product

$$N_e(\lambda, \varphi, h) = VTEC(\lambda, \varphi)F(h) \qquad (1)$$

where λ is the geographic longitude and φ is the geographic latitude associated to any measurement taken during a particular RO. Using the IAT method the RO-retrieved shape functions are determined up to the altitude of the LEO satellite orbit, which is between 700 and 800 km in the case of the CF3 constellation.

STIP model fit

The topside ionosphere region is mainly populated by a mixture of two ions, O^+ and H^+, among other ion species that are significantly less abundant. The O^+ ion population dominates in the topside ionosphere, while the H^+ ion is the most abundant in the plasmasphere. Based on these considerations, the STIP model is used to distinguish between the ionospheric and the plasmaspheric contribution to the VTEC. For each RO from our sample, the STIP model function [4]

$$F_{\text{fit}}(h) = Ae^{-h/h_s} + B \qquad (2)$$

is fit to the retrieved shape function $F(h)$ in the range of altitudes going from 400 km to nearly the CF3 satellite altitude. The STIP model assumes that the ionospheric electron density gradient in the topside-ionosphere region corresponds to the density gradient of the O^+ ion, and that the O^+ density follows an exponential decay represented by the first term in equation (2), where h_s is the vertical scale height of decay and A is a proportionality factor that measures the magnitude of the topside-ionosphere density. To ensure that the exponential function can be used to represent the density gradient of the O^+ ion, a lower-limit altitude of 400 km for the fitting region has been chosen because, in general, it is sufficiently above the F2-peak altitude [4].

Additionally, the STIP model assumes that the plasmaspheric electron density gradient, corresponding to the density gradient of the H^+, is negligible in the range of altitudes used in the fits. The true H^+ ion density slowly decays with altitude from its maximum value, but the vertical scale height of decay is typically at least one order of magnitude greater than h_s. Taking into account that the interval of altitudes used in the fits has a size of 300-400 km, the expected variation of H^+ will be really low and, consequently, the H^+ density can be approximated by the constant parameter, B, appearing in the second term of equation (2).

The STIP model has been shown to provide an accurate representation of the electron density in the topside-ionosphere region [4], improving the best-fits achieved by other classical model functions (Chapman, Epstein or single exponential functions). A comparison of the distribution of the mean deviations, Δ_r, between different best-fit model functions and observations is shown in Figure 1 for a sample of electron density profiles calculated during 2009. In 80% of cases the STIP model achieves mean deviations less than 4% with regard to actual profiles in the region going from 400 and 700 km of altitude.

Ionospheric and plasmaspheric electron contents

After deriving the best-fit values of the STIP model parameters (A, h_s and B) for the different shape functions calculated with the IAT method from our sample of ROs, the ionospheric electron content, EC_{ion}, is calculated by adding two contributions. The first contribution comes from the altitude integral of the RO-retrieved electron density profile given by equation (1). This integral is calculated from the minimum altitude sampled by the RO (about 100 km) till the lowest altitude used by the STIP model fit (set to 400 km). Then, the second contribution (arising from the topside-ionosphere region) is calculated as the altitude integral of the VTEC times the exponential term in equation (2), starting at 400 km. This latter integral can be extended upward the CF3 satellite altitude with an effective upper limit of infinity. An example of the procedure is illustrated in Figure 2. Note that the exponential decay is very fast for altitudes greater than the UTH, since the scale height values, h_s, found from the fits are between 50 and 200 km in more than 90% of the cases [4].

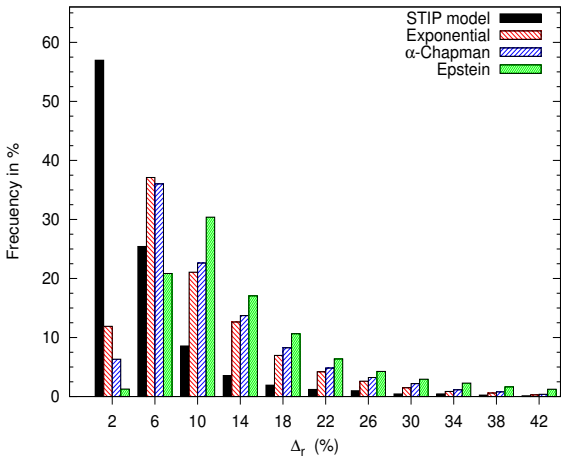

Figure 1: Histogram of the distribution of mean %-deviations in the topside-ionosphere region between different best-fit models and RO-derived electron density profiles.

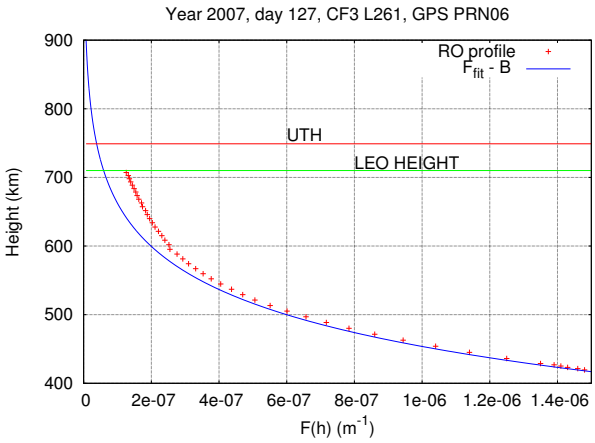

Figure 2: An example of the extrapolation strategy used to calculate EC_{ion}. Red crosses: a particular RO-retrieved shape function. Blue solid line: the extrapolated exponential term from equation (2) obtained after fitting the STIP model function. The red and green horizontal lines indicate, respectively, the UTH derived by the STIP model and the height of the CF3 satellite.

Finally, after having calculated EC_{ion}, the plasmaspheric electron content, EC_{pl}, is calculated as the difference:

$$EC_{\mathrm{pl}}(\lambda,\varphi) = VTEC(\lambda,\varphi) - EC_{\mathrm{ion}}(\lambda,\varphi) \quad (3)$$

Note that the proposed procedure to separate the VTEC into EC_{ion} and EC_{pl} is not based on using a specific altitude to perform such separation, but in taking into account implicitly (through the use of the STIP model) the particular value of the UTH for each individual electron density profile (see next section). In this sense, our method follows a different approach from previous studies based on direct measurements of the electron content taken from a nearly constant LEO satellite altitude (e.g., [2], [7]), where this altitude is used to separate the ionospheric and plasmaspheric electron contents. In these studies, the results are associated to the particular altitude of the LEO satellite orbit and when this altitude is higher than the UTH, the topside-ionosphere contribution to EC_{ion} will be overestimated while the resulting EC_{pl} will be severely underestimated.

Upper transition height

The best-fit values A, h_s and B to the different shape functions from our sample can be used to determine the UTH (hereafter denoted as H_u), characterizing the boundary between the ionosphere and the plasmasphere and defined as the altitude where the O^+ and H^+ ion densities are equal. From this definition and assuming that the O^+ and H^+ ion densities are represented by the first and second terms in the right side of equation (2), the following relationship is inferred [4]:

$$H_u = h_s \ln(A/B) \quad (4)$$

Figure 3 shows the frequency distribution during 2009 of the H_u values calculated from equation (4). One can see that the distribution has a large dispersion (from 350 to more than 1000 km). Specifically, in nearly 80% of cases H_u is found to be below the typical altitude of CF3 satellites (750-800 km). This demonstrates the importance of achieving in the topside-ionosphere region a reliable separation of the VTEC into the ionospheric and plasmaspheric contributions, which is the purpose of the STIP model fit by means of equation (2). If instead of doing this separation, one directly counts all the electron content below the CF3 orbit as belonging to the ionosphere, then part of the plasmaspheric electron content is frequently included in the resulting value of EC_{ion}. This may give rise to a severe underestimation of EC_{pl}, particularly when the UTH is low, since the bottom-side plasmasphere (that will be erroneously assumed as part of the ionosphere) makes the largest contribution to the plasmaspheric electron content.

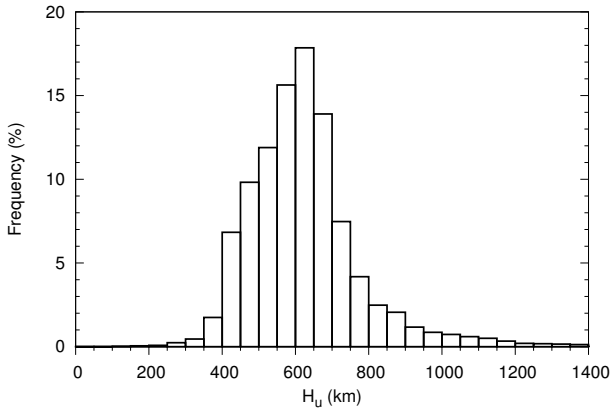

Figure 3: Histogram of the frequency distribution of the UTH.

RESULTS

Testing the performance of the method

The pairs of values EC_{ion} and EC_{pl} derived from our sample have been used to assess the performance of the method. To this end, we have analyzed the well-known ionospheric anomalies (see [8] for details) and the detection of the annual anomaly in the plasmasphere in the South-American sector of longitudes [2].

In Figure 4, the local time (LT) variation of the mean ionospheric and plasmaspheric electron contents during the December and June solstices and the March equinox is presented for low and intermediate geomagnetic latitudes in the Northern and Southern geomagnetic hemispheres. The semi-annual anomaly in the ionosphere (electron content during the March equinox, around midday, greater than during the December solstice) can be clearly observed although with a noticeable hemispheric asymmetry. In the Southern hemisphere it is less prominent than in the Northern one. This is consistent with observations and model results for the last solar minimum period [9]. On the other hand, the annual anomaly (the electron content around midday combined from both hemispheres is greater during December solstice than during June solstice) is also present in the ionosphere, but again a clear hemispheric asymmetry is seen in the results presented in Figure 4. In particular, it is evident that the annual anomaly is due essentially to a larger difference between the EC_{ion} values in December and June in the South hemisphere than in the North hemisphere.

From Figure 4, one can also observe the reversal of the seasonal anomaly in the ionosphere. The seasonal anomaly is characterized by greater electron content during local winter than during local summer in each hemisphere. However, during solar minimum periods this anomaly reverses and the electron content during local summer becomes greater than during local winter [8], [9]. Indeed, this is seen for intermediate geomagnetic latitudes where the summer/winter differences are more significant

in general. Nevertheless, for low geomagnetic latitudes the reversal is also observed in the Southern hemisphere while in the Northern hemisphere the reversal is not complete. This is also consistent with the previous study by [8].

Figure 4 shows that the main contribution to the VTEC in the central hours of the day comes from the ionosphere. Since the annual, semi-annual and seasonal anomalies have been previously detected using the VTEC [11], it may not be surprising that the different anomalies can also be detected in the ionospheric electron content. Hence, a much more interesting test for our method is the analysis of the results for EC_{pl}.

The Earth's magnetic field typically connects the ionospheric F-region at middle latitudes with the equatorial plasmasphere along the magnetic field lines. According to some studies [2], this ionosphere-plasmasphere coupling can give rise to some LT variation in the low-latitude plasmasphere, especially for quiet periods of solar and geomagnetic activity, as it is the case for our data sample. In particular, after the ionospheric electron content has increased during the morning, an upward flow of plasma from the mid-latitude ionosphere following the Earth's magnetic field lines will fill the magnetic flux tubes at higher altitudes reaching the plasmasphere in the equatorial region. Indeed, an indication of the effects of this plasma flow can be observed in Figure 4, where the low-latitude plasmaspheric electron content during the solstices and the March equinox (Fig. 4, left column) starts increasing between 8:00 and 10:00 LT, a few hours after the enhancement of the mid-latitude ionospheric electron content has started (Fig. 4, right column).

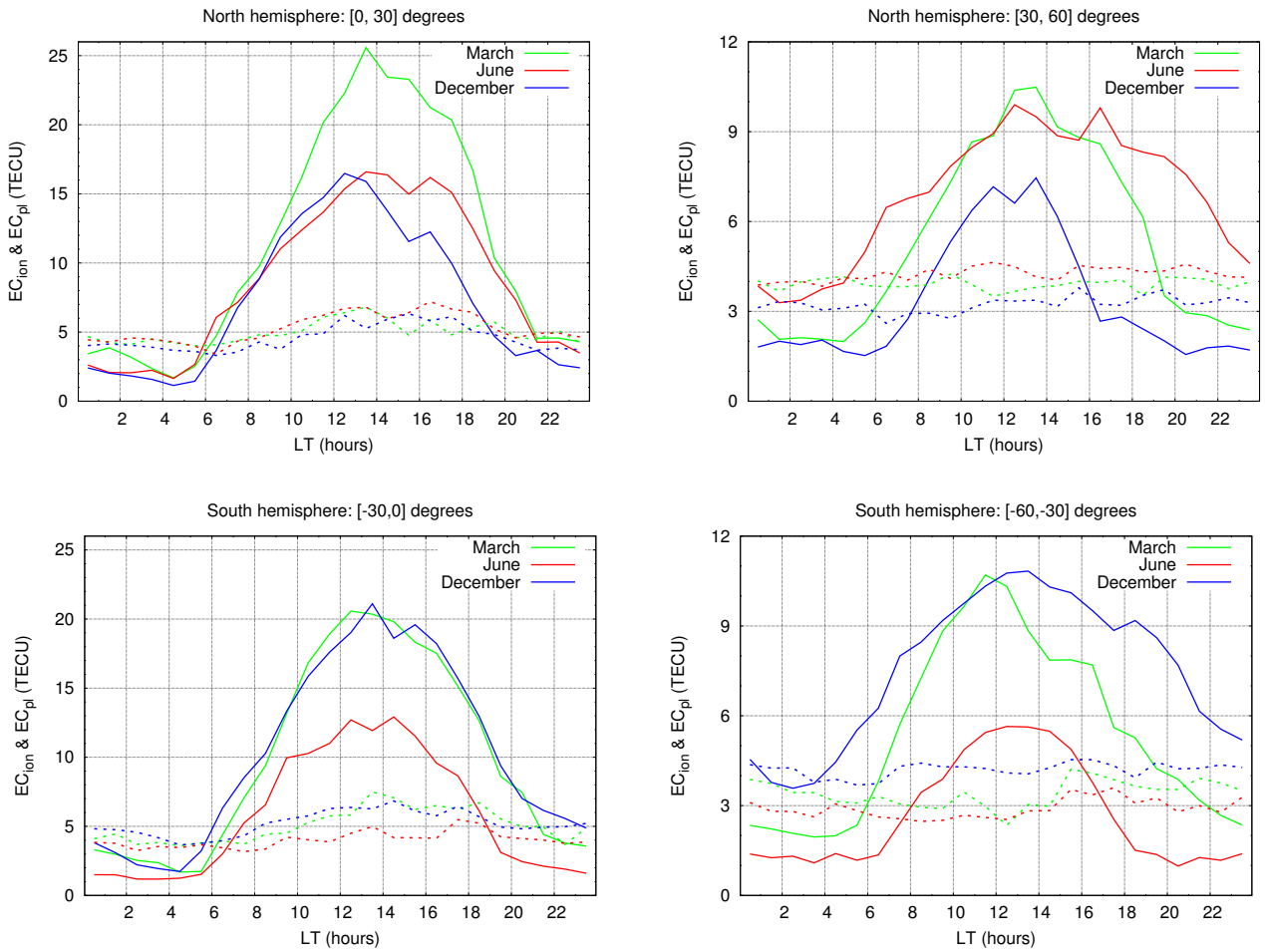

Figure 4: The LT variation of the hourly mean electron content in the ionosphere (solid lines) and the plasmasphere (dotted lines) for low (left column) and intermediate (right column) geomagnetic latitudes in each hemisphere during the June and December solstices and the March equinox.

On the contrary, the mid-latitude plasmasphere does not show any LT evolution, keeping more or less constant along the day. A more detailed view of the LT variation of EC_{pl} in the region around the geomagnetic equator is presented in Figure 5, where one can observe that during the solstice corresponding to the local summer in each hemisphere, the LT variation of the equatorial EC_{pl} has a wider shape (corresponding to a longer duration of the sunlight period, and an early sunrise) than during the local-winter solstices in each hemisphere. This is the same behavior as seen in the mid-latitude EC_{ion} during the same periods of the year in both hemispheres (Fig. 4, right column). Hence, the results from Figure 5 are consistent with the existence of a flow of ionized material connecting the mid-latitude ionosphere with the equatorial plasmasphere, as has been claimed in other studies [2].

Another plasmaspheric trend that can be used to test the results of EC_{pl} derived from our method is the existence of an annual anomaly in the equatorial plasmasphere during the day. This anomaly has been observed in the longitudinal sector covering South-America [2], [10], while no evidence of the semi-annual anomaly exists. Figure 6 shows the longitudinal variation of the low-latitude plasmaspheric electron content for the central hours of the day during the solstices and the March equinox. The annual anomaly is present in the interval of longitudes between, approximately, 200 and 300 degrees, covering the South-American continental region, while the semi-annual anomaly is not observed. Moreover, the ratio between the December and June electron contents in that sector of longitudes is in the range of 1.5 to 2.0. All these results are in agreement with previous studies [2], [10].

Ionosphere-plasmasphere interplay

Figures 4 to 6 have confirmed that our method is able to reproduce previously known features in the ionosphere and plasmasphere. The relationship between EC_{pl} and EC_{ion} is of great interest to characterize the coupling and interplay of the ionosphere-plasmasphere system. In this section, a more detailed investigation of this relationship is performed by analyzing the fractional electron content in the ionosphere, $ION_f = EC_{ion}/VTEC$.

It is evident that the magnitude of the ION_f variations will be significantly smaller than the EC_{ion} variations, since the former is a fractional quantity. The variations of ION_f will be mostly driven by the large variations observed in the ionospheric electron content (see Figure 4), but typical trends of the fractional ionospheric electron content can be immediately associated to trends in the fractional plasmaspheric electron content, $PL_f = EC_{pl}/VTEC$, through the relationship:

$$ION_f + PL_f = 1 \qquad (5)$$

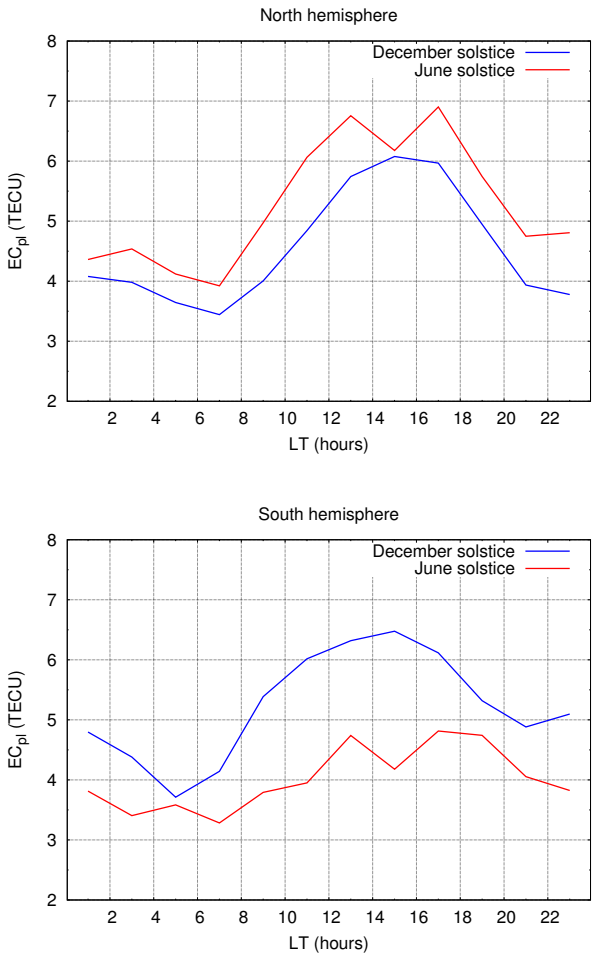

Figure 5: The LT variation of the equatorial plasmasphere (±30° around the geomagnetic equator) in the Northern and Southern hemispheres during the solstices.

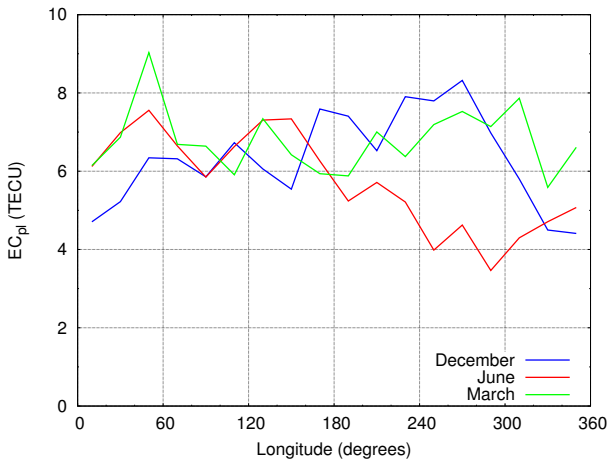

Figure 6: Longitudinal variation of the plasmaspheric electron content during the solstices and the March equinox for a latitudinal band of 20 degrees centered in the geomagnetic equator and for the sunlight period from 10:00 to 16:00 LT.

Figure 7 shows a preliminary study of the frequency distribution (during summer and winter in 2007) of ION_f. One can see that the values of the fractional electron content in the ionosphere have a similar distribution in both seasons, with nearly the same median and peak values (around 0.7). In fact, about 75% of the measurements are within the range 0.6-0.8, suggesting that the midday variation of ION_f was not very large during 2007.

Figure 8 shows a more detailed analysis of the LT variations of ION_f during summer and winter seasons for two different geomagnetic latitude intervals and in the two Earth hemispheres. One can see that the maximum mean value of ION_f (approximately equal to 0.7) is always achieved around midday, being similar in all the cases shown in the figure. The minimum value of ION_f occurs just before sunrise LT and is smaller around the geomagnetic equator than for mid-latitude. Sunrise LT in each graph of Figure 8 approximately coincides with the starting time of the ION_f enhancement from its minimum value. This enhancement clearly traces the recovering of the daytime ionosphere as the solar zenith angle decreases after sunrise. The ionosphere reaches a level of maximum ionization nearly at midday, when the solar zenith angle is minimum.

One can also observe in Figure 8 that the slope of the LT variation of ION_f during a few hours after sunrise is similar in summer and winter seasons, but it is different for the middle and equatorial geomagnetic latitude ranges. In order to model this particular trend, the following function has been considered to fit the LT variation of ION_f between sunrise and midday:

$$ION_f(t) = I_{\max} - De^{-(t-t_s)/\tau_i} \qquad (6)$$

where t indicates the LT, t_s is the time of sunrise at 350 km of altitude (sunrise has been considered at a representative altitude of the F layer), and $D = I_{\max} - I_s$ being the difference between the maximum and minimum values achieved by ION_f, with $I_s = ION_f(t_s)$. Note that we have set $I_{\max} = 0.7$ (in accordance with the results shown in Figures 7 and 8), so equation (6) has two free parameters, namely, D (or equivalently, I_s) and τ_i, this last parameter corresponding to the timescale of development of the daytime ionosphere.

Figure 9 displays some examples of the best-fit curves (black solid lines) to the ION_f values derived from our sample of ROs (red crosses). The data used for the fits cover the period of solar light from t_s to approximately 13:00 LT. As can be seen, the model function is able to reproduce the typical LT variation in ION_f between sunrise and midday. Specifically, the median deviation (in absolute value) between data points and best-fit curves is approximately 10% in all the cases analyzed.

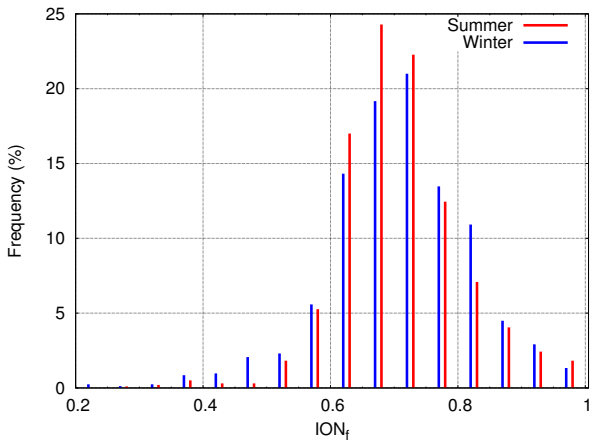

Figure 7: Frequency distribution of the fractional electron content in the ionosphere at the North hemisphere (from 0 to 60 degrees of geomagnetic latitude) and around midday (LT interval from 11:00 to 15:00).

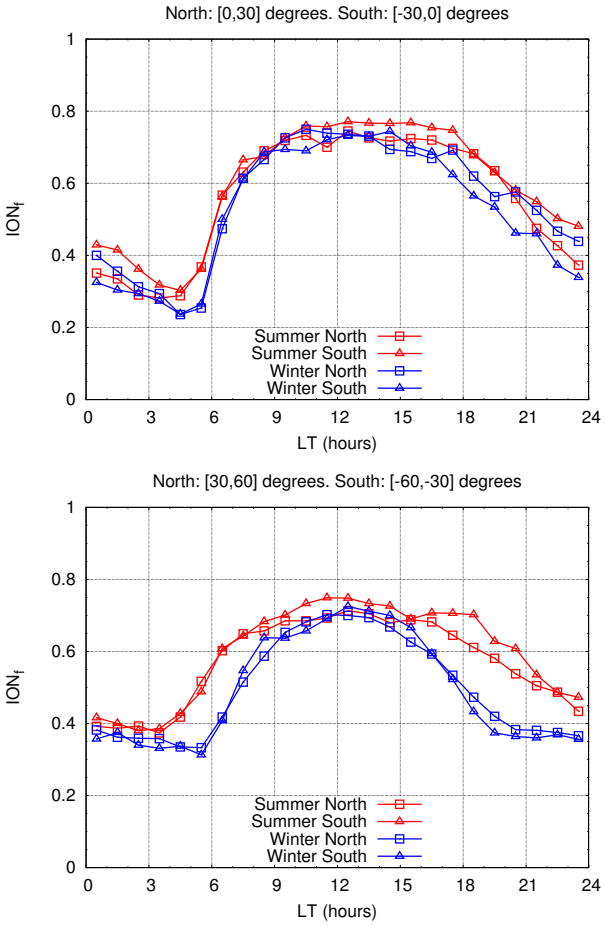

Figure 8: LT variation of the hourly-mean value of ION_f during the summer and winter seasons in the Northern and Southern hemispheres.

Tables 1 and 2 show the best-fit parameters for the different geomagnetic latitude bands considered, in different hemispheres and for local summer and winter periods. The geomagnetic latitude dependence of the best-

fit parameters is evident in both Tables. In particular, the fractional VTEC in the ionosphere at sunrise, I_s, clearly increases with geomagnetic latitude, while the timescale, τ_i, decreases as the latitude range considered approaches the geomagnetic equator, implying a faster development of the daytime F layer near the equatorial band than at intermediate latitudes. In general the summer/winter difference between the best-fit values in Tables 1 and 2 is low and almost negligible compared with the variations that can be observed among different geomagnetic-latitude ranges. These quantitative results confirm the trends previously observed in Figure 8.

DISCUSSION

It is remarkable that the maximum mean value reached by ION_f during the 24-hour period (Figure 8) is approximately the same (about 0.7) and occurs around noon, for the two geomagnetic-latitude ranges considered and for summer and winter. This implies a nearly constant minimum value of PL_f at the same period of the day and, consequently, an approximately constant ratio between the ionospheric and the plasmaspheric electron contents around noon along the year, regardless of the geomagnetic latitude considered. This indicates the existence of a significant coupling between the electron contents in the ionosphere and the plasmasphere during the low solar activity period analyzed. This coupling deserves a more detailed analysis for different solar activity periods to confirm if it corresponds to some general trend of the ionosphere-plasmasphere system.

The LT variations of ION_f calculated from our data sample show that the plasmasphere has a greater relevance than the ionosphere during the night. In particular, just before sunrise the plasmasphere makes the largest contribution to the VTEC. This contribution can be nearly 75% of the VTEC around the geomagnetic equator and during winter. The minimum value of ION_f is smaller for low geomagnetic latitudes than in the mid-latitude region (see Table 2). There are several reasons that may explain this latitudinal difference of I_s. For instance, the electrodynamics of the equatorial ionosphere has important effects on ION_f and, particularly, **E**×**B** drifts at low latitudes during the nighttime are responsible of a downward ion drift that gives rise to a reduction of the equatorial density, while during the daytime the upward ion drift enhances the density in that region [9]. In this way, a larger contrast between the day and night ION_f values should be expected for low latitudes than for middle latitudes, as it is seen in Table 2 and in Figure 8. Another effect that may contribute to reduce the value of I_s from middle to low geomagnetic latitudes is the downward plasma flux during the night from the equatorial plasmasphere toward the mid-latitude ionosphere [2]. This plasma flux will enhance the pre-sunrise values of ION_f at intermediate geomagnetic latitudes.

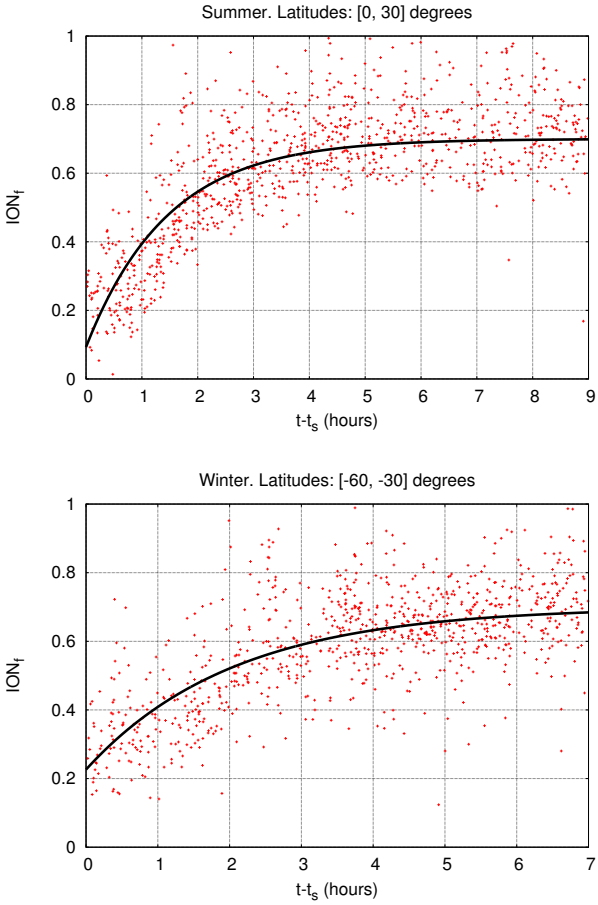

Figure 9: Two examples of best-fit curves (black solid lines) to ION_f values (red crosses). The horizontal axis is the time after sunrise at 350 km of altitude.

Table 1: Best-fit values of timescale τ_i in hours

Geomagnetic Latitude:	*Summer*	*Winter*
[30°,60°]	2.2	2.4
[0°,30°]	1.5	1.2
[-30°,0°]	1.4	1.3
[-60°,-30°]	1.9	2.1

Table 2: Best-fit values of parameter I_s (minimum ION_f)

Geomagnetic Latitude:	*Summer*	*Winter*
[30°,60°]	0.26	0.29
[0°,30°]	0.09	0.03
[-30°,0°]	0.14	0.11
[-60°,-30°]	0.24	0.23

Finally, the timescale τ_i of development of the daytime ionosphere has a marked latitudinal dependence (according to Figure 8 and Table 1), while for a given range of geomagnetic latitudes it is very similar between the two seasons of the year that have been analyzed. The faster development of the daytime equatorial ionosphere can be explained by the faster variation of the solar zenith angle after sunrise in this region. The time taken by the Sun to reach a given elevation is longer as the geographic latitude increases and, for this reason, during the first hours of the day the effects of the photoionization from the Sun will be noticeable near the equator faster than at intermediate and high latitudes. Consequently, one should expect that the timescale τ_i increases as the geographic latitude increases during summer and winter, but having similar values in both seasons. Although in Figure 8 and Table 1 the data are grouped into intervals of geomagnetic (instead of geographic) latitude, this effect can still be observed.

CONCLUSIONS

A method that allows the calculation of the electron content in the ionosphere and the plasmasphere from ROs and VTEC measurements has been presented. The method self-consistently combines the IAT inversion technique for electron density retrieval, ground measurements of the VTEC and adequate modeling of the topside-ionosphere electron density. In this way, the ionospheric and plasmaspheric electron contents can be derived by modeling the actual UTH value and without relying on an artificial boundary imposed by the fixed satellite altitude from which the measurements are taken. Applying this method to RO measurements from the CF3 satellite constellation and VTEC data from IGS GIMs, a global analysis of the plasmaspheric and ionospheric contributions to VTEC has been performed for a period of low solar and geomagnetic activity. The performance of the method has been demonstrated by reproducing several results from previous studies for the recent solar minimum period, namely, the disappearance of the seasonal anomaly, the existence of an annual anomaly not only in the ionosphere but also in the plasmasphere (specifically in the South-American sector of longitudes) and, finally, showing that the semi-annual anomaly in the ionosphere is more prominent in the Northern than in the Southern hemisphere.

Our results also show that the contribution of the plasmasphere is, in general, significant and can even be the main contribution to the VTEC, particularly before dawn for low and intermediate geomagnetic latitudes. The ionosphere develops more abruptly (with a shorter timescale) and from a lower level of fractional electron content as the geomagnetic latitude decreases. However, the maximum value of ION_f (and the corresponding minimum value of PL_f) is typically the same for all ranges of geomagnetic latitudes considered and for summer and winter periods, the maximum being always achieved around noon, when the ionosphere reaches the state of maximum ionization. This implies that the ratio between the electron contents of the ionosphere and the plasmasphere around midday is quite constant, suggesting the existence of an important coupling between both regions.

The different results previously described require further analysis to characterize in more detail the different dependencies of ION_f that have been observed (for example, considering different periods of solar activity). The methodology introduced in the present work certainly opens the possibility of conducting studies of the ionosphere-plasmasphere system at a global scale, which may ultimately lead to an improvement in the modeling of this coupled system. In particular, it has been shown that the model function given by equation (6) (with two free parameters) can be used to describe the typical time variation of the electron content during the development of the daytime ionosphere. For that period of time, equation (6) provides a simple tool to quickly calculate first-order approximations of the separate ionosphere and plasmasphere contributions from current VTEC maps. From this simple model one can develop more complex mapping functions taking into account the relevance of the plasmaspheric contribution to the VTEC and improving the reliability of current GIMs based on the assumption that the only contribution to VTEC measurements arises from the ionosphere.

ACKNOWLEDGMENTS

The authors would like to thank the University Corporation for Atmospheric Research, the National Space Organization in Taiwan and CDAAC for making available the CF3 constellation data. We also thank IGS for the availability of their IONEX-format files from which VTEC values have been calculated.

REFERENCES

[1] Sanz, J., Juan, J. M., and Hernández-Pajares, M. (2013), *GNSS Data Processing. Vol. 1: Fundamentals and Algorithms*. ESA communications, ESTEC TM-23/1, Noordwijk, the Netherlands

[2] Lee, H.-B., G. Jee, Y. H. Kim, and J. S. Shim (2013), "Characteristics of global plasmaspheric TEC in comparison with the ionosphere simultaneously observed by Jason-1 satellite", *Journal of Geophysical Research Space Physics*, Vol. 118, pp. 935-946, doi: 10.1002/jgra.50130

[3] Schaer, S., Gurtner, W., and Feltens, J. (1998) IONEX: The IONosphere Map Exchange Format Version 1. In: *Proceeding of the IGS AC Workshop*, Darmstadt, Germany, pp 233–247

[4] González-Casado, G., Juan, J. M., Hernández-Pajares, M., and Sanz, J. (2013), "Two-component model of topside-ionosphere electron density profiles retrieved from Global Navigation Satellite Systems radio occultations", *Journal of Geophysical Research. Space Physics*, Vol. 118, pp. 7348-7359, doi: 10.1002/2013JA019099

[5] Hernández-Pajares, M., Juan, J. M., and Sanz, J. (2000), "Improving the Abel inversion by adding ground GPS data to LEO radio occultation in ionospheric sounding", *Geophysical Research Letters*, Vol. 27, No. 16, pp. 2473-2476

[6] Aragon-Angel, A., Y.-A. Liou, C.-C. Lee, B. W. Reinisch, M. Hernández-Pajares, J. M. Juan, and J. Sanz (2011), "Improvement of retrieved FORMOSAT-3/COSMIC electron densities validated by ionospheric sounder measurements at Jicamarca", *Radio Science*, Vol. 46, RS5001, doi:10.1029/2010RS004578

[7] Pedatella, N. M., J. M. Forbes, A. Maute, A. D. Richmond, T.-W. Fang, K. M. Larson, and G. Millward (2011), "Longitudinal variations in the F region ionosphere and the topside ionosphere-plasmasphere: Observations and model simulations", *Journal of Geophysical Research*, Vol. 116, A12309, doi:10.1029/2011JA016600

[8] Lee, W. K., H. Kil, Y.-S. Kwak, Q. Wu, S. Cho, and J. U. Park (2011), "The winter anomaly in the middle-latitude F region during the solar minimum period observed by the Constellation Observing System for Meteorology, Ionosphere, and Climate", *Journal of Geophysical Research*, Vol. 116, A02302, doi: 10.1029/2010JA015815

[9] Nanan B., C. Y. Chen, P. K. Rajesh, J. Y. Liu, and G. J. Bailey (2012), "Modeling and observations of the low latitude ionosphere-plasmasphere system at long deep solar minimum", *Journal of Geophysical Research*, Vol. 117, A08316, doi:10.1029/2012JA017846

[10] Menk, F. W., S. T. Ables, R. S. Grew, M. A. Clilverd, and B. R. Sandel (2012), "The annual and longitudinal variations in plasmaspheric ion density", *Journal of Geophysical Research*, Vol. 117, A03215, doi: 10.1029/2011JA017071

[11] Liu, L., W. Wan, B. Ning, and M.-L. Zhang (2009), "Climatology of the mean total electron content derived from GPS global ionospheric maps", *Journal of Geophysical Research*, Vol. 114, A06308, doi: 10.1029/2009JA014244